32nd Annual International Conference of the IEEE EMBS
Buenos Aires, Argentina, August 31 - September 4, 2010

EXPERIMENTAL DEMONSTRATION OF NONCONTACT PULSE WAVE VELOCITY MONITORING USING MULTIPLE DOPPLER RADAR SENSORS

Li Lu, Changzhi Li, and Donald Y. C. Lie

Department of Electrical and Computer Engineering, Texas Tech University, Lubbock, Texas, 79409, USA
Email: changzhi.li@ttu.edu

Abstract — In this paper, two Doppler radars are used to monitor the pulse movements at the heart and the calf in order to measure the pulse wave velocity (PWV) wirelessly. Both simulation and experiment have been performed to demonstrate the feasibility of the proposed noncontact PWV monitoring. A three-stage calibration procedure, including DC offset calibration, circuit delay calibration and antenna radiation pattern calibration, has been developed for reliable long-term PWV monitoring. The measurement results have been verified by wired contact measurement with pulse transducers.

Index Terms — Doppler radar, noncontact, arctangent demodulation, calibration, pulse wave velocity, healthcare.

I. INTRODUCTION

Pulse wave velocity (PWV) has been studied for decades and the capability of long-term monitoring of patients' PWV is very important for the healthcare industry. Bazzett found that PWV is related to the artery blood pressure in 1922 [1]. Since then much attention has been paid on the non-invasive continuous monitoring of blood pressure by analyzing the PWV. Besides, PWV has been demonstrated as an independent predictor of diseases such as hypertension, vascular damages, diabetics with presumed atherosclerosis, and end-stage renal failures [2].

Traditionally, electrocardiogram (ECG) and other wired medical instruments are used to measure pulse waveforms at two locations (e.g., carotid-femoral PWV, brachial-ankle PWV). The transit time T is obtained from the phase difference of the two pulse waveforms, and the pulse wave travelling distance S is estimated. Therefore, PWV can be easily calculated by dividing S with T. However, the conventional methods rely on contact-based wired technologies and the probes and wires confine the activities of the subject to be measured, making it inconvenient for long-term monitoring of patients' health conditions. Also, the surface-loading effect and body fluid such as sweat can reduce the accuracy of contact-based measurement [3].

Recently, Doppler noncontact vital signs detection has attracted wide interests from the microwave and healthcare community [4]~[8]. Based on the Doppler phase modulation effect, a Doppler radar can sense the physiological movement (usually the respiration and the heartbeat) without any probe attached to a human body, which makes the vital sign detection much more flexible and attractive for long-term monitoring [4]. Subsequently, the feasibility of using Doppler radars to detect PWV without anything attached to the human body has been theoretically studied [5]. In this paper, two Doppler radars are used in experiment to monitor the pulse movements at the heart and the calf. The *I*/*Q* baseband signals are sampled by an NI USB6009 data acquisition module (DAQ). The arctangent demodulation technique [6] is adopted to obtain the phase information from the heartbeat and calf pulse movement. Experiments have demonstrated that reliable PWV can be measured using the noncontact Doppler radar technology.

This paper is organized as follows: Section II introduces the theory of Doppler noncontact physiological movement detection and PWV measurement. Simulation results of the Doppler noncontact measurement of PWV are presented in section III. Section IV reports experimental results. A conclusion is drawn in Section V.

II. THEORY

A. Noncontact Physiological Movement Detection

Based on the Doppler theory, a target with a time varying position but a net zero velocity will reflect the signal with its phase modulated proportional to the time-varying target position [7]. A Doppler radar typically transmits a single-tone continuous electromagnetic wave $T(t) = \cos(2\pi ft+\varphi(t))$, where f is the local oscillator frequency, t is the elapsed time, and $\varphi(t)$ is the phase noise of the oscillator. The signal is reflected by a subject at a nominal distance d_0 with a time-varying displacement $x(t)$, and the total distance traveled between the transmitter and the receiver is $2d(t) = 2d_0+2x(t)$. The received signal can be approximated as [7]:

$$R(t) \approx \cos\left[2\pi ft - 4\pi x(t)/\lambda - 4\pi d_0/\lambda + \varphi(t - 2d_0/c)\right] \quad (1)$$

where c is the signal's propagation velocity (the speed of light) and λ is the wavelength of the signal in air, which is equal to c/f. For a quadrature receiver, the baseband I and Q signals after down-conversion can be approximated as:

$$B_I(t) = A_I \cos\left[\theta + 4\pi x(t+\Delta t)/\lambda + \Delta\varphi\right] \quad (2)$$

$$B_Q(t) = A_Q \sin\left[\theta + 4\pi x(t+\Delta t)/\lambda + \Delta\varphi\right] \quad (3)$$

where A_I and A_Q are the amplitude of the I and Q signals, which will be the same if the amplitude mismatch between the two channels is calibrated out. θ is a constant phase shift

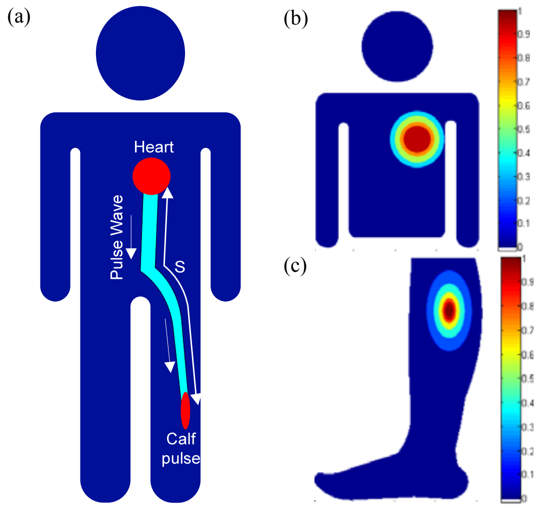

Fig. 1. Ray-tracing model for noncontact PWV monitoring. (a) Pulse wave propagating from the heart to the calf with a transmit distance of *S*. (b) Modeling of the normalized amplitude of physiological movement caused by the heartbeat (c) Modeling of the normalized amplitude of physiological movement caused by the calf pulse.

due to the distance d_0 and the reflection at the surface, Δt is the time delay accumulated in the receiver baseband circuit, and $\Delta\varphi$ is the random phase noise of the radars. $4\pi x(t)/\lambda$ is the phase information due to the physiological movement and is linearly proportional to the displacement of the subject being measured. Since there are DC offsets in both channels due to reflections from stationary objects (clutters) and hardware imperfections, Eqs. (2) and (3) should be modified to:

$$B_I(t) = \cos\left[\theta + 4\pi x(t+\Delta t)/\lambda + \Delta\varphi\right] + DC_I \quad (4)$$

$$B_Q(t) = \sin\left[\theta + 4\pi x(t+\Delta t)/\lambda + \Delta\varphi\right] + DC_Q \quad (5)$$

where it is assumed that the I/Q amplitude mismatch has been calibrated out. The accurate phase information can be obtained by arctangent demodulation [6] if the DC offsets are properly calibrated out:

$$\psi(t) = \arctan\left[\frac{B_Q(t)}{B_I(t)}\right] + F = \theta + \frac{4\pi x(t+\Delta t)}{\lambda} + \Delta\varphi \quad (6)$$

where F is a multiple of 180^0 for the purpose of eliminating the discontinuity when $\psi(t)$ crosses the boundary of two adjacent quadrants in the constellation graph [8]. Once the demodulated phase is obtained from (6), the motion of the subject is known.

B. Pulse Wave Velocity Measurement

The heartbeats pulsate through the arteries as the heart serves as the source of vibrations. The transient phases of a pulse wave at different locations along an artery are different, due to the different distances from the heart. The phase difference is related to the pulse wave transit time T from one location to the other. Based on the estimated distance S between the two locations, the mean PWV can be calculated as $v = S/T$. Fig. 1 (a) illustrates the approach of PWV measurement.

Assume that the two pulse movements are denoted as $x_1(t)$ and $x_2(t)$, both of which have the same periodicity as the heartbeat. Two Doppler radars will be used to monitor the pulses at two locations. According to Section II-A, the phase-demodulated baseband output of the two radars can be obtained after DC calibration as:

$$\psi_1(t) = \theta_1 + 4\pi x_1(t+\Delta t_1)/\lambda_1 + \Delta\varphi_1 \quad (7)$$

$$\psi_2(t) = \theta_2 + 4\pi x_2(t+\Delta t_2)/\lambda_2 + \Delta\varphi_2 \quad (8)$$

where θ_1 and θ_2 are the constant phase shifts due to the nominal distance from the radar to the subject, Δt_1 and Δt_2 are the delays in the receiver circuits, $\Delta\varphi_1$ and $\Delta\varphi_2$ are the random phase noise of the oscillators. The random phase noise of the oscillator $\Delta\varphi$ is effectively suppressed by the range correlation effect [7], and is neglected in the following discussion. Since θ_1 and θ_2 add constant values to the demodulated phase, it shifts the demodulated waveform up or down without affecting the shape and delay of the phase waveforms. If the difference between Δt_1 and Δt_2 can be calibrated, the phase delay between the two pulses (pulse wave propagating time) can be recovered by comparing the two waveforms of $\psi_1(t)$ and $\psi_2(t)$.

C. Calibration

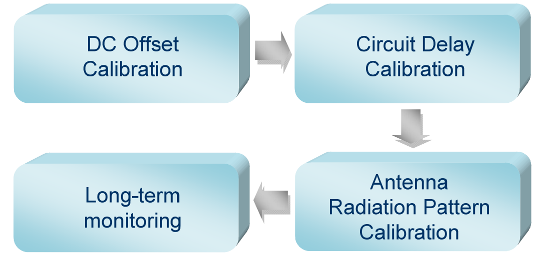

Fig. 2. Three-step calibration procedure for long-term PWV monitoring.

In order to obtain accurate detection, a three-step calibration is necessary as shown in Fig. 2. First, *DC offset calibration* is performed for reliable arctangent demodulation of the phase information. Second, since the baseband circuit in the radar receiver introduces delay which is in the same scale as the signal of interest, a *circuit delay calibration* is needed to eliminate the difference between Δt_1 and Δt_2 in (7) and (8). Finally, since the antenna has a finite directivity, an *antenna radiation pattern calibration* is needed to correct the distance between the effective radiation centers of the two antennas.

The DC offset calibration can be performed with the help of constellation graph [8]. For circuit delay calibration, a linear actuator will be used to provide a reference movement for the two radars simultaneously, and then the difference in the delays of the two radars can be aligned. The antenna radiation pattern calibration will be performed with the help of two contact pulse transducers which provide the pulse information from two fixed positions on the subject. The

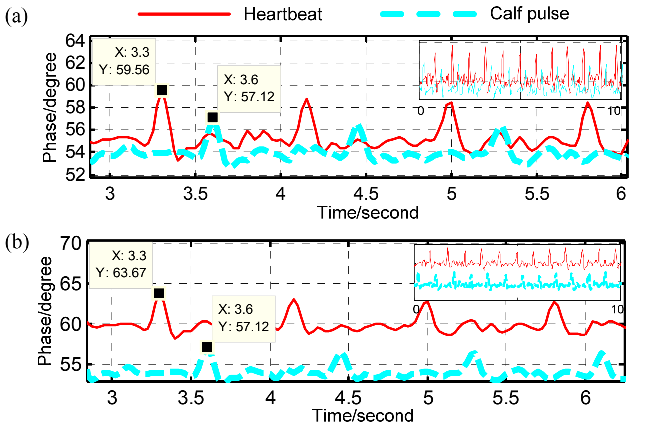

Fig. 3. Simulated pulse wave detected by: (a) Two Doppler radars both at 20 cm away from the heart center and the calf. (b). Two Doppler radars at 45 cm and 20 cm away from the heart center and the calf, respectively.

results measured by the radar will be compared with those by the pulse transducers to calibrate out the error caused by finite antenna directivity.

After the calibrations, the phase delay T between $\psi_1(t)$ and $\psi_2(t)$ is only decided by the phase delay between the pulses at two specific locations, making the noncontact PWV measurement possible. Both simulation and experiments will be performed to verify the feasibility of Doppler noncontact PWV measurement.

III. Simulation

Ray-tracing model was used to simulate the Doppler noncontact PWV measurement. An 80 cm upper body and a 40 cm long calf were modeled as shown in Fig. 1 (b) and Fig. 1 (c). The normalized amplitudes of physiological movement caused by the heartbeat and the calf pulse are also shown on the plots. As a first order approximation, the skin of the chest and the calf is assumed to be uniform. A 6.05 GHz Doppler radar is placed in front of the chest facing the heart center, while another 5.64 GHz Doppler radar faces the calf pulse center. The pulse waveform detected by a pulse transducer (UFI 1010) was used. The transit time of the pulse wave from the heart to the calf is assumed to be 0.3 second in the simulation.

Two sets of simulations were performed. In the first simulation, the distances from each of the two radars to their respective subject were both 20 cm. In the second simulation, the distances were 45 cm and 20 cm respectively. As shown in Fig. 3, the time delay between the heartbeat and the calf pulse always indicates a 0.3 second propagating time from the heart to the calf pulse location. The change of the detecting distances only affects the base level of the detected phase. Based on the estimated heart-calf vessel distance, which is approximately 1.0 meter, the simulated PWV is around 3.3 m/s.

IV. Experiment

Experiments have been performed to measure the heart-to-calf PWV. Two quadrature Doppler radars were designed and fabricated on printed circuit board (PCB). The carrier frequencies were tuned to 6.05 GHz and 5.63 GHz

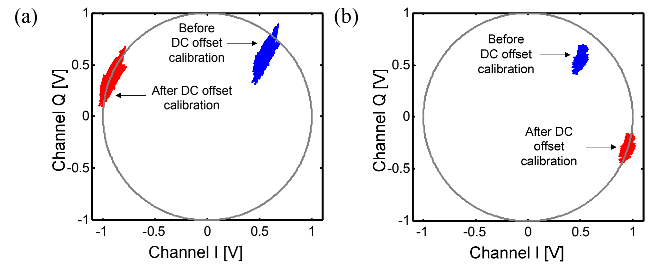

Fig. 4. Constellation plot of I/Q signals for DC calibration. (a) heartbeat (b) calf pulse.

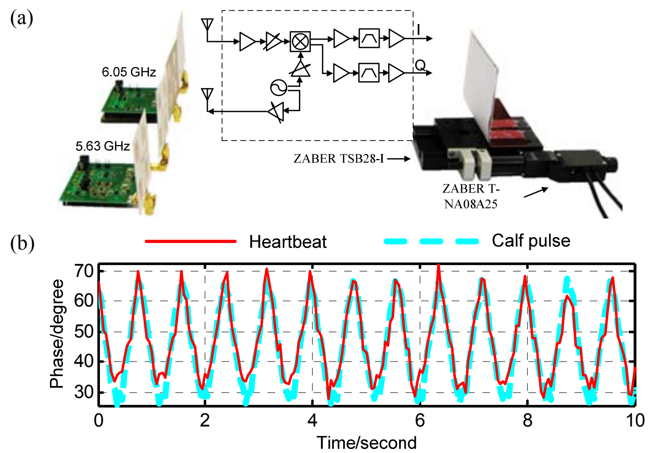

Fig. 5. (a) Set up of the circuit delay calibration using a linear actuator. (b) Arctangent demodulated phase information when the linear actuator was programmed to generate a periodic single-tone movement.

respectively. The Doppler radar with a carrier frequency of 5.63 GHz detected the calf pulse while the one with a carrier frequency of 6.05 GHz monitored the heartbeat. The carrier frequencies of the two radars are set to be different so that the interference between the two radars can be eliminated. The detecting distances will be changed to verify that the phase shift due to the detecting distance does not affect the measured PWV. In the mean time, two pulse transducers (UFI 1010) were attached to the chest wall and the calf to provide a reference. The baseband output of the two radars as well as the pulse transducer data were sampled by an NI USB6009 data acquisition module (DAQ) and were sent to a laptop with LabVIEW for real-time signal processing.

In order to obtain clear time domain waveform of the calf pulse, the calf was laid on a hard surface so that the blood vessels were compressed and the physiological movement was signified. The breath of the subject was held still for most of the time to reduce interference caused by the harmonics of breathing signal.

The DC offsets was first compensated properly before the arctangent demodulation to recover correct phase information. Constellation plots of I/Q data before and after the DC calibration were presented in Fig. 4 to verify the effectiveness of DC offset calibration.

In order to calibrate the signal delay in the electronic circuit, a set of linear actuator (ZABER T-NA08A25) and linear translation stage (ZABER TSB28-I) was placed in front of the two radars to provide a reference movement, as shown in Fig. 5 (a). Since the two radars were monitoring the same object, the phase difference between the two

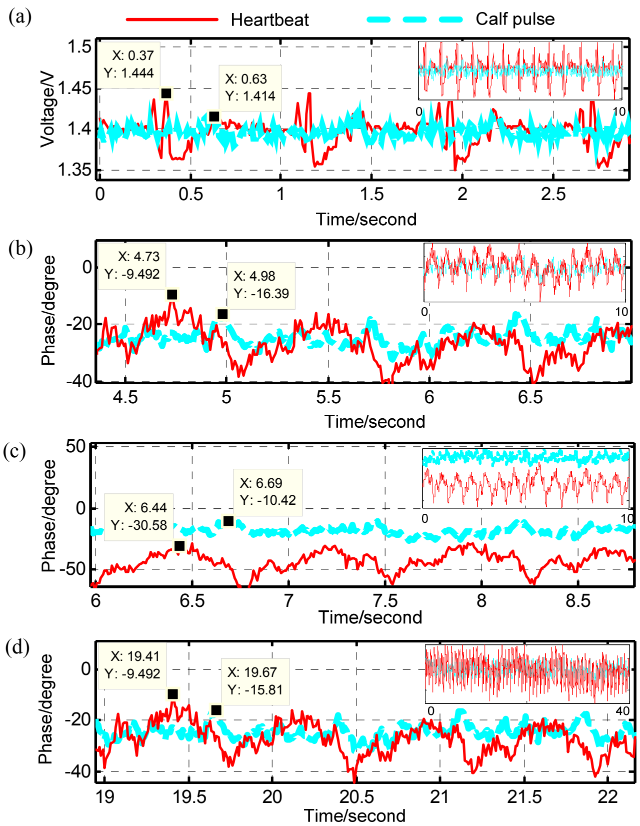

Fig. 6. Experimental results of PWV measurement. (a) Reference signal provided by the pulse transducers. (b) Radar measurement result. (c) Radar measurement result at a different detecting distance. (d) Long-term monitoring after the antenna radiation pattern calibration.

TABLE I
LONG-TERM MONITORING RESULTS COMPARISON

Time(sec)	Reference PWV(m/s)	Noncontact PWV(m/s)	Error
135	4.000	4.167	4.18%
235	3.704	3.846	3.83%
488	4.348	4.000	8.00%
868	3.704	3.846	3.84%
Average value	3.939	3.965	0.65%

arctangent-demodulated waveforms is decided by the delay in the receiver circuit. Therefore, the difference in the electronic circuit delay can be calibrated out. Fig. 5 (b) presents the arctangent-demodulated baseband phase information. A 0-second time delay between the peaks of the two curves was obtained.

The output data from radars and transducers were compared to perform the antenna radiation pattern calibration. Figs. 6 (a) and (b) show the reference phase information of the pulse waveforms obtained by the pulse transducers, and the phase information detected by the Doppler radars after the arctangent demodulation, respectively. The contact pulse transducer measures a reference pulse wave transit time of 0.260 s from the heart to the calf. If the pulse wave travelling distance is estimated as 1 meter, the reference average heart-calf PWV is 3.85 m/s. The arctangent demodulation result shows clear phase delay between the two detected signals. The average pulse wave transit time is calculated as 0.253 s. The 0.007 s error caused by the antenna radiation pattern is then identified and calibrated out.

Different detection distances were also tested. The demodulated waveform at a different detection distance is shown in Fig. 6 (c). Comparing Figs. 6 (b) and (c), it is shown that the pulse wave propagating time holds almost the same. Therefore, it is verified that the phase shift due to the detecting distance does not affect the PWV measurement result.

Long-term PWV monitoring of over 15 minutes was performed after the calibrations. Fig. 6(d) shows the a short period waveform during the long-term monitoring. The pulse wave propagating time is carefully calculated in each period and the average value is around 0.26 s. Table I reports some instantaneous data during the long-term PWV monitoring. The error between the results obtained from the noncontact Doppler radar vs. those of the wired-sensor is smaller than 10 %, while the error between the averaged results is only 0.65 %. It should be noted that the average result is more important for long-term PWV measurement. The error is mainly due to random body movement and quantization error.

V. CONCLUSION

A new method of noncontact PWV measurement has been developed based on the Doppler phase modulation effect. It has been verified by experiments in an engineering lab setting. Arctangent demodulation with DC offset compensation is used in this study. The error caused by the antenna radiation pattern is calibrated out carefully before reliable long-term PWV monitoring. Experiments show that the heart-to-calf PWV can be successfully measured using the Doppler noncontact radar technology.

REFERENCES

[1] H. C. Bazzett and N. B. Dreyer, "Measurement of pulse wave velocity", *J. Am. Physiol*, vol. 63, pp. 94-116, Dec. 1922.

[2] R. Asmar, *Arterial stiffness and pulse wave velocity: clinical application*, Paris, France: Elsevier, 1999.

[3] H. Vermarien and E. va Vollenhoven, "The recording of heart vibrations: a problem of vibration measurement on soft tissue," *Medical and Biological Engineering and Computing*, vol. 22, no. 2, pp. 168-178, 1984.

[4] C. Li, J. Cummings, J. Lam, E. Graves, and W. Wu, "Radar remote monitoring of vital signs", *IEEE Microwave Magazine*, vol. 10, issue 1, pp. 47-56, February 2009.

[5] L. Lu, C. Li, and D. Y. C. Lie, "Microwave Noncontact Measurement of Pulse Wave Velocity for Healthcare Applications", *11th Annual IEEE Wireless and Microwave Technology Conference*, Melbourne, FL, April 2010.

[6] B. Park, O. Boric-Lubecke, and V. M. Lubecke, "Arctangent demodulation with DC offset compensation in quadrature Doppler radar receiver systems," *IEEE Trans. Microw. Theory Tech.*, vol. 55, pp. 1073-1079, May 2007.

[7] A. D. Droitcour, O. Boric-Lubecke, V. M. Lubecke, J. Lin, and G. T. A. Kovac, "Range correlation and I/Q performance benefits in single-chip silicon Doppler radars for noncontact cardiopulmonary monitoring", *IEEE Trans. Microw. Theory Tech.*, vol. 52, pp. 838-848, Mar. 2004.

[8] C. Li, and J. Lin, "Random Body Movement Cancellation in Doppler Radar Vital Sign Detection", *IEEE Trans. Microw. Theory Tech.*, vol. 56, No. 12, pp. 3143-3152, Dec. 2008.